[3]J. T. Vallin, G. A. Slack, S. Roberts, and A. E. Hughes, Phys. Rev. B 2, 4313 (1970).
[4]G. A. Slack, F. S. Ham, and R. M. Chrenko, Phys. Rev. 152, 376 (1966).
[5]P. Kovacs and E. Lendvay (unpublished).
[6]B. Clerjaud and B. Lambert, J. Phys. E 4, 619 (1971).
[7]D. Smith and J. H. M. Thornley, Proc. Phys. Soc. (London) 89, 779 (1966).
[8]J. L. Prather, Natl. Bur. Std. Monograph No. 19 (U. S. GPO, Washington, D. C., 1961).
[9]A. Räuber and J. Schneider, Z. Naturforsch. 17a, 266 (1962).
[10]R. S. Title, Phys. Rev. 131, 623 (1963).
[11]R. Parrot and G. Tronche, Phys. Status Solidi 41, 217 (1970).
[12]W. M. Walsh, Jr., Phys. Rev. 122, 762 (1961).
[13]W. M. Walsh, Jr. and L. W. Rupp, Jr., Phys. Rev. 126, 952 (1962).
[14]J. Schneider, S. R. Sircar, and A. Räuber, Z. Naturforsch. 18a, 980 (1963).
[15]B. Lambert, T. Buch, and B. Clerjaud, Solid State Commun. 10, 25 (1972).
[16]J. Dieleman, R. S. Title, and W. V. Smith, Phys. Letters 1, 334 (1962).
[17]B. Lambert, T. Buch, and P. Jaszczyn-Kopec, Compt. Rend. 271B, 1232 (1970).
[18]W. M. Walsh, Jr., Phys. Rev. 114, 1473 (1959).
[19]G. Pfister, W. Dreybrodt, and W. Assmus, Phys. Status Solidi 36, 351 (1969).
[20]I. T. Steinberger (private communication).
[21]O. Brafman and I. T. Steinberger, Phys. Rev. 143, 501 (1966).
[22]H. Nelkowski and O. Pfützenreuter, Acta Cryst. A 27, 296 (1971).
[23]C. Barthou, Compt. Rend. 271B, 966 (1970).
[24]D. Curie and C. Barthou, Compt. Rend. 272B, 473 (1971).
[25]R. R. Sharma, T. P. Das, and R. Orbach, Phys. Rev. 149, 257 (1966).
[26]R. R. Sharma, Phys. Rev. B 3, 76 (1971).
[27]G. H. Azarbayejani, Ph. D. thesis (The University of Michigan, 1966) (unpublished).
[28]H. Watanabe and H. Kishishita, Progr. Theoret. Phys. (Kyoto) Suppl. 46, 1 (1970).
[29]T. Buch and A. Gelineau, Phys. Rev. B 4, 1444 (1971).

PHYSICAL REVIEW B VOLUME 7, NUMBER 1 1 JANUARY 1973

Conversion of Electromagnetic into Acoustic Energy via Indium Films*

A. Zemel and Y. Goldstein
The Racah Institute of Physics, The Hebrew University, Jerusalem, Israel
(Received 3 August 1972)

Transverse acoustic waves were generated electromagnetically at 9 GHz using thin indium films on silicon substrates. We report measurements of the conversion efficiency α of electromagnetic into acoustic energy as a function of temperature, magnetic field, and microwave power. The highest conversion efficiency found above the superconducting transition temperature T_c of indium was 5×10^{-5} comparable to that of quartz transducers. Below T_c the conversion efficiency decreases rapidly and becomes magnetic field and microwave power dependent. At low powers a good agreement was found between the experiment and the theory of Abeles with respect to both the value and temperature dependence of α. This agreement shows that the generation of the acoustic waves is due primarily to diffuse scattering of electrons at the surfaces of the film. To fit the theory to the experiment we had to assume that diffuse surface scattering persists below T_c as well and thus we conclude that pair scattering at the surface does not conserve momentum. In addition, our results show that α is still appreciable at temperatures well below T_c and thus transverse-phonon generation may possibly be one of the important loss mechanisms in superconducting cavities.

I. INTRODUCTION

An electromagnetic field in the GHz region incident on a metal film can generate a transverse acoustic wave. The ions and electrons in the metal are accelerated by the electromagnetic field within the penetration depth. For a clean thin film at low temperatures, scattering in the bulk can be neglected, and thus the interaction of the electromagnetic field with the lattice ions may result in the generation of an acoustic wave. There may be another, electronic, contribution to the generation of an acoustic wave. Assuming diffuse surface scattering, the momentum gained from the electromagnetic field by the electrons is transferred to the lattice at the surfaces. This momentum per unit time is a shear force acting on the surface and can also give rise to a transverse acoustic wave.

Experimentally, electromagnetic generation of acoustic waves using indium films was first observed by Abeles[1] and later by the present authors.[2] Theoretically, the problem of electromagnetic generation of transverse acoustic waves in a metal has received considerable attention over the last few years. To calculate the conversion ef-

ficiency of the process, most of the authors[3-7] considered mainly the direct electromagnetic force on the lattice ions. For frequencies in the GHz range, these calculated conversion efficiencies are much too low and/or do not reproduce the experimental temperature dependence. Abeles[1] and later Southgate[8] included, in addition to the direct electromagnetic force, the force on the ions arising from the scattering of electrons at the metal surface. Abeles considered a simplified model of a thin film, neglected the electronic scattering within the film, and assumed diffuse surface scattering. Southgate considered a semi-infinite metal but included bulk scattering and allowed for partially specular surface scattering. In the limit of long mean free path and diffuse surface scattering, the two calculations are in good agreement and yield conversion efficiencies comparable to our experimental values.

According to the theory of Abeles, there is a sharp decrease in the conversion efficiency of electromagnetic to acoustic energy upon the transition of the metal (in this case, indium) film from the normal into the superconducting state. Thus it seems natural to study this phenomena around the superconducting transition temperature T_c. In this paper we present measurements of the conversion efficiency as a function of temperature, microwave power, and dc magnetic field, both above and below T_c.

II. EXPERIMENTAL

Indium films, 1100–1500 Å in thickness, were vacuum deposited on optically polished high-purity silicon rods. The axis of the rods was along either the [110] or [100] direction and their end faces were parallel within 6″ of arc. The dimensions of the rods were about 0.95 cm in diameter and 1.27 cm in length. The silicon face with the indium film on it was pressed against a 0.6-cm-diam hole in the bottom wall of a high-Q resonant rectangular microwave cavity. To ensure an optimal contact between the indium film and the cavity wall, the area around the hole was also indium coated. The whole arrangement was immersed in liquid helium and the temperature could be varied by reducing the vapor pressure. The cavity was excited with 9.02-GHz microwave pulses of 1-μsec duration, 150-W maximum peak power, and 5×10^{-5} duty cycle. The power reflected and/or radiated from the cavity was detected by a superheterodyne receiver, and displayed on an oscilloscope as a function of time.

Because of the microwave excitation pulse, a pulse of acoustic wave is generated by the indium film. The acoustic pulse propagates along the silicon rod, is reflected at each end face, and bounces back and forth in the silicon rod. Each time the acoustic wave reaches the cavity, part of the acoustic energy is reconverted into microwave energy (by the indium film) and an electromagnetic echo pulse is radiated from the cavity. Thus, each microwave excitation pulse is followed by a train of echo pulses. This is illustrated by the oscillogram in Fig. 1. The first pulse arises from partial reflection of the excitation pulse at the cavity and is orders of magnitude higher than the succeeding echo pulses. The spacing of successive echoes corresponds to twice the time of flight of the acoustic wave through the silicon rod. In the experiments performed with silicon rods whose axis was along the [110] direction, two sets of echoes were observed corresponding to the fast and slow shear waves in silicon.

Usually five to seven echoes were observed in the temperature range from 4.2 K down to the superconducting transition temperature of indium (3.4 K). The echo amplitude decreased exponentially with 7–10-dB attenuation between successive echoes. A typical plot of echo power (in dB) versus the time t is shown in Fig. 2, where $t=0$ corresponds to the application of the microwave excitation pulse. We define the insertion loss (IL) as the ratio of the echo power extrapolated to $t=0$, to the microwave input power. The conversion efficiency α, on the other hand, is defined as the ratio of the *acoustic power* to the microwave input power. To generate an echo two conversion processes are necessary. First, electromagnetic energy has to be converted into sound energy, and second, at a later time, sound energy has to be reconverted into electromagnetic energy. The two processes are symmetrical and thus, if the properties of the indium film remain unchanged

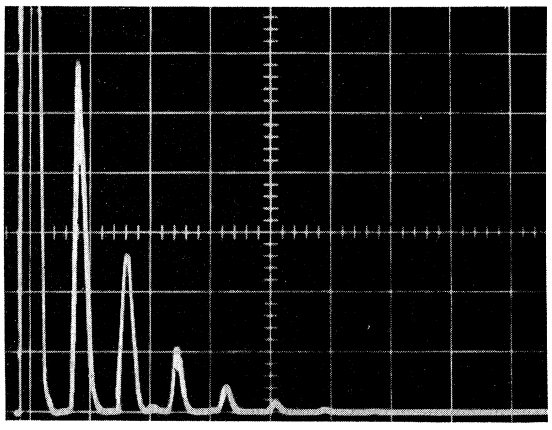

FIG. 1. Typical oscillogram of echoes detected by the superheterodyne receiver above T_c. Horizontal scale, 5 μsec/division.

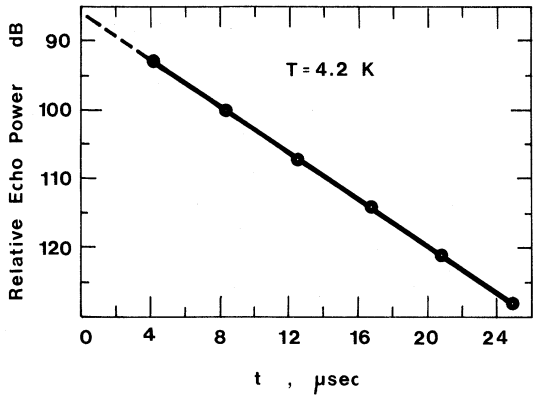

FIG. 2. Typical plot of echo power (in dB) vs time t, at $T = 4.2$ K; $t = 0$ corresponds to the application of the microwave excitation pulse.

during this time interval, $\alpha^2 = \text{IL}$. As will be shown below, this is not always the case.

A. Power Dependence

In Fig. 3 the power dependence of IL in dB is plotted as a function of the microwave input power at different temperatures T. The microwave power is expressed in dB as well, and 0 dB corresponds to the maximum power (≈ 150 W). Above the superconducting transition temperature T_c of indium, IL was found to be power independent. This is illustrated in Fig. 3(a) (4.2 K). Figures 3(b)–3(d) show the power dependence below T_c. In Fig. 3(b) ($T/T_c = 0.97$), the insertion loss at the highest microwave power (0 dB) has the same value (86 dB) as above T_c. At somewhat lower powers IL decreases rapidly to about 90.5 dB. At this value the data show a shoulder and IL remains constant as the power decreases. At still lower powers IL again decreases rapidly until it attains a constant value at low powers. In Fig. 3(c) ($T/T_c = 0.93$), IL starts already at a value (89 dB) somewhat below its value above T_c, but the general behavior is similar to that in Fig. 3(b). We see again a shoulder which is now narrower, and a rapid decrease on both sides of the shoulder region. The constant value at low powers was not attained in this measurement. The data in Fig. 3(d) ($T/T_c = 0.88$) show mainly a narrow shoulder region which starts already at high powers.

The power dependence of IL was interpreted as follows. At the arrival of the high-power microwave pulse, the superconducting film is quenched and becomes normal. At temperatures close to T_c, at the highest powers the film acts as normal even at the generation of the first echo pulse (and sometimes also the second one). Thus the measured IL is the same as above T_c and is equal to α_n^2, where α_n is the conversion efficiency of indium in the normal state. As the power is decreased, the indium film becomes gradually superconducting at the time of the echo pulse. Hence IL decreases (increases in dB) until it eventually becomes equal to $\alpha_n \alpha_s$, where α_s is the conversion efficiency of superconducting indium. Decreasing the power further does not affect IL (the shoulder region) until a power level is reached at which the indium is not completely quenched any more at the arrival of the excitation pulse. Now IL again decreases with decreasing power until it attains its final value α_s^2. At somewhat lower temperatures IL was below α_n^2 even at 0 dB [see Figs. 3(c) and 3(d)]. In addition, the sensitivity of our instruments was not always enough to determine the final value of IL $= \alpha_s^2$. However, the shoulder region was always observable and could thus serve to determine α_s.

The power dependence of IL in our first experiments was somewhat different and is shown in Fig. 4. As can be seen in Fig. 4(a), at the highest powers the value of IL is close to α_n^2 even at $T/T_c = 0.77$. In addition, both curves exhibit local maxima at the power levels where one expects the completion of the superconducting transitions. It was established that these maxima were connected with a substantial improvement in the cavity Q. This

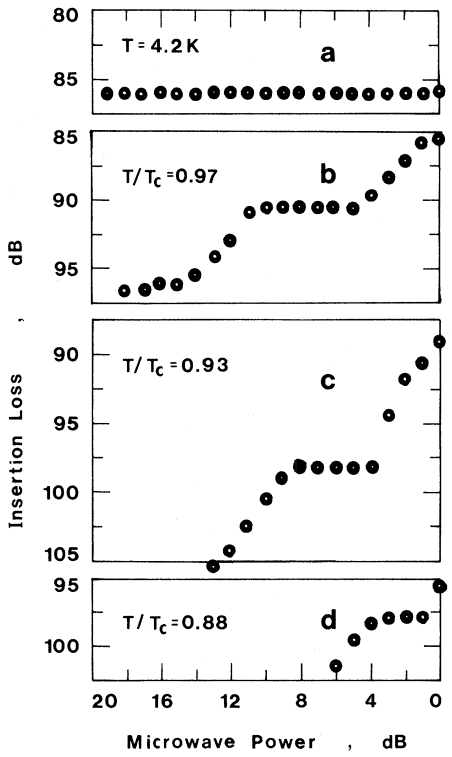

FIG. 3. Dependence of IL on microwave input power at different temperatures. 0 dB on the abscissa corresponds to the maximum microwave power (≈ 150 W).

improvement could not be explained simply by the change of the surface impedance of the indium film (which is part of the cavity wall). We believe that in these experiments the contact between the indium film and the rest of the cavity wall was somewhat lossy, thus reducing the Q of the cavity. Upon transition into the superconducting state, the contact losses decreased resulting in a higher Q. After improving our arrangement of pressing the Si crystal against the cavity wall, these side effects disappeared.

B. Temperature Dependence

The measurements were performed in the temperature range 4.2–1.4 K. Above the superconducting transition temperature (3.4 K) the amplitude of the echoes was found to be temperature independent. The attenuation between successive echoes and the absolute value of the insertion loss varied somewhat from sample to sample. The latter was attributed to variation in the cavity Q, the contact between the film and the cavity wall, and variations in film thickness. The best insertion loss measured above T_c was 86 dB. Thus our highest conversion efficiency was $\alpha_{nM} = 5\times 10^{-5}$ (43 dB).

Below T_c the insertion loss becomes strongly temperature (and power) dependent. This is shown in Fig. 5. As pointed out above, the absolute value of IL varied somewhat from sample to sample. To compare the temperature dependence obtained with different samples, the points in Fig. 5 were computed as follows. For each sample we plotted the ratio $(\alpha_s/\alpha_n)^2$, i.e., the insertion loss in the superconducting state relative to that in the normal state. This ratio was then normalized to the best insertion loss measured above T_c, α_{nM}^2. Thus α_s^2 in Fig. 5 stands for $(\alpha_s/\alpha_n)^2\alpha_{nM}^2$.

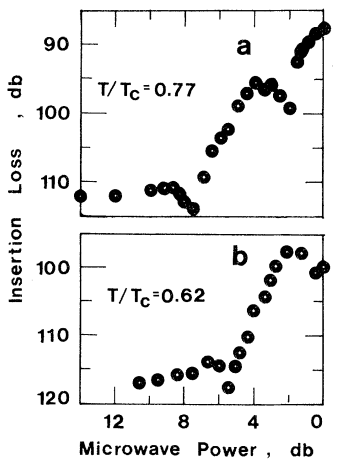

FIG. 4. Power dependence of IL for another sample at two temperatures. The local maxima (and minima) exhibited by the data were attributed to a substantial increase in the cavity Q upon the transition of the film into the superconducting state.

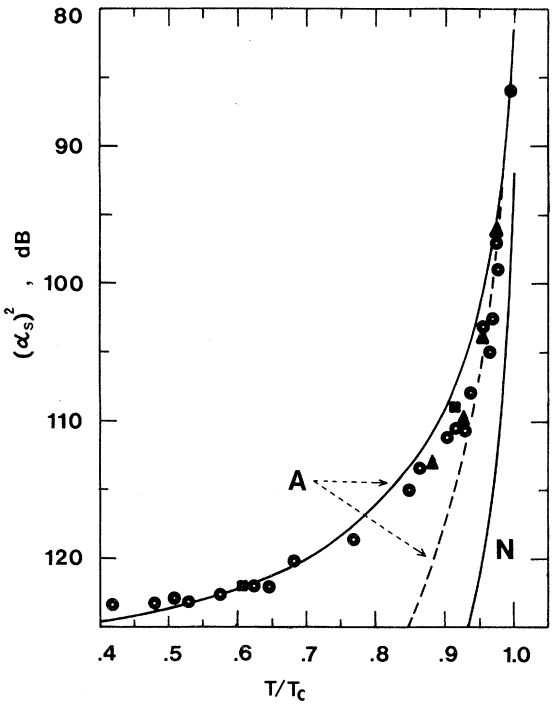

FIG. 5. Measured conversion efficiency squared α_s^2 vs reduced temperature T/T_c. The points were obtained from the value of IL at low powers, the triangles from the shoulder region of the IL-vs-power curves, and the squares from measurements on outlying echoes, as explained in the text. The theoretical curves labeled A are for the case of the extreme anomalous limit and curve N for the case of normal skin effect. The two solid curves were calculated on the assumption that $n/n_0 = 1$. In calculating the dashed curve, a two-fluid model was assumed for the temperature dependence of n/n_0.

To evaluate α_s from the measured IL we usually used the value of IL at very low powers, where IL becomes power independent. The values obtained by this method are represented by the points in Fig. 5. The triangles in Fig. 5 were obtained from the value of IL in the shoulder region as explained above. The two additional points (squares) were obtained from the temperature dependence of the third through fifth echo and will be discussed below. As can be seen in the figure, the values obtained by the different methods (as well as on different samples) are in good agreement. The lines in the figure are theoretical, calculated under different assumptions and will be explained in Sec. III.

C. Magnetic Field Dependence

To generate the magnetic fields we used solenoids immersed in liquid nitrogen on the outside of the

liquid-helium Dewar. For fields perpendicular to the film surface a single solenoid was used with vertical axis. For the parallel-field measurements, a pair of Helmholtz coils was used. Our maximum fields were about 1 kOe.

Above the superconducting transition temperature of the indium films no dependence on the magnetic field was observed. Below T_c, on the other hand, the echo amplitude was very sensitive to the presence of a magnetic field. At temperatures and powers where the amplitudes of the echoes were below that obtained with "normal" indium, the application of a magnetic field always restored them to the normal value. The strength of the field required to attain the normal value was temperature dependent and usually also microwave power dependent. This is illustrated in Fig. 6, where an echo amplitude (in arbitrary units) is plotted versus the applied (perpendicular) magnetic field. The two lines correspond to different values of the microwave power P. We define a microwave-power-dependent critical field $H_c(T, P)$ as the minimum field necessary to restore the normal conversion efficiency (see Fig. 6). At low microwave powers, $H_c(T, P)$ approaches a limit as shown in Fig. 7. Here we plotted the values for perpendicular fields of $H_c(T, P)$ as a function of the microwave power. We identify the limiting value of $H_c(T, P)$ at low powers with the critical field of the film, $H_c(T)$. Figure 8 shows the temperature dependence of $H_c(T)$. The squares represent measurements with a parallel magnetic field. The lower data (points and triangles) were obtained with a perpendicular field on two samples of somewhat different thicknesses. The lines were calculated from the theory of Tinkham[9] and will be

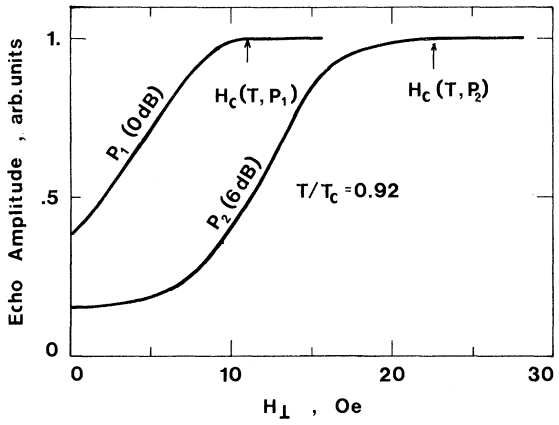

FIG. 6. Dependence of echo amplitude (in arbitrary units) on applied (perpendicular) magnetic field at $T/T_c = 0.92$. The two lines correspond to different values of the microwave power P. The values of $H_c(T, P)$ are indicated by the arrows in the figure.

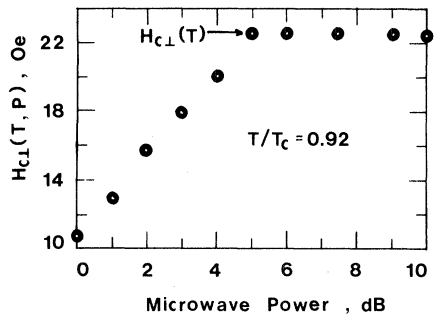

FIG. 7. Dependence of $H_{c\perp}(T, P)$ (perpendicular fields) on microwave power at $T/T_c = 0.92$. The limiting value at low powers $H_{c\perp}(T)$ is indicated by the arrow.

discussed in Sec. III.

In the high- and intermediate-power range, where $H_c(T, P)$ was microwave power dependent, the value of $H_c(T, P)$ depended also on the particular echo which was measured. The reason for this can be understood as follows. The generation of the acoustic wave depends only on the state of the indium film at the time of the microwave excitation pulse. The generation of the echo pulses by the acoustic wave depends, however, on the state of the indium film at the time of each echo. It may

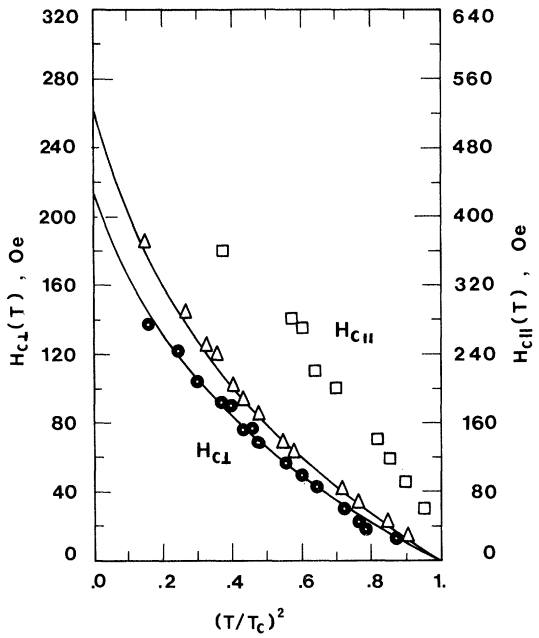

FIG. 8. Values of $H_c(T)$ as a function of the reduced temperature. The upper data represent measurements with parallel fields. The lower data represent measurements with perpendicular fields on two samples of somewhat different thicknesses d (circles, $d = 1400$ Å; triangles, $d = 1200$ Å). The curves were calculated from the theory of Tinkham (Ref. 9).

happen that at the time of the first echoes, the film acts normal or is in an intermediate state, and only at the later echoes is the indium film truly superconducting. The critical field $H_c(T, P)$ is thus expected to increase as a function of echo number until it reaches the limiting value of $H_c(T)$. This is shown in Fig. 9, where we plotted $H_{c\perp}(T, P)$ as a function of echo number at $T = 0.72T_c$. The data for Fig. 9 were taken with the full microwave power ($\simeq 150$ W). As can be seen from the figure, in this case the first echo acts normal even in the absence of a magnetic field. The field required to quench the indium film at the time of succeeding echoes progressively increases and saturation starts only at the fourth echo. With lower microwave powers this saturation moved to smaller echo numbers.

The fact that the outlying echoes are generated by superconducting indium provides another means for measuring α_s. If at the time of the microwave excitation pulse the film is normal, then the ratio of the echo power of a "late" echo to that of the same echo with indium in the normal state yields α_s/α_n. To ensure that at the time of the generation of the *acoustic* wave the film is really normal, one applies enough power so that the amplitude of the *first* echo equals that produced by normal indium. As an example, we plotted in Fig. 10 the relative echo power of the different echoes at $T = 0.61T_c$. The data represented by the triangles were measured without a magnetic field while the circles were measured in a magnetic field above the critical field. As can be seen in the figure, the first echo is independent of the magnetic field (i.e., acts normal in zero field). Measurements of $H_c(T, P)$ for the different echoes

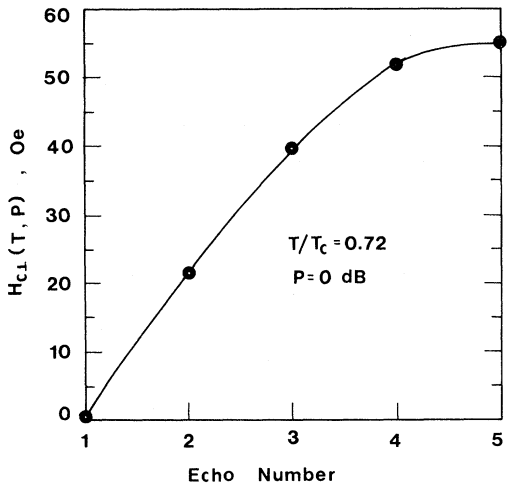

FIG. 9. $H_{c\perp}(T, P)$ as a function of echo number at $T = 0.72T_c$. The data were taken with the full microwave power ($\simeq 150$ W).

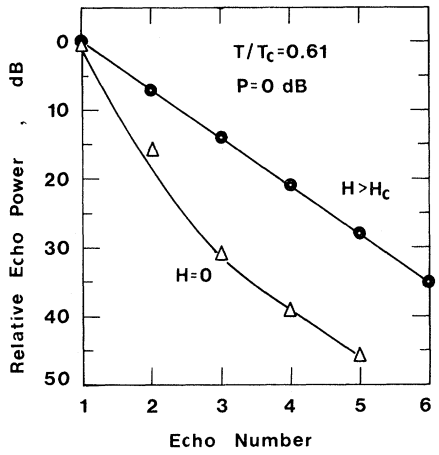

FIG. 10. Relative echo power vs echo number. Triangles represent measurements in the absence of a magnetic field, while the points represent measurements with a magnetic field $H > H_c(T)$.

showed that from the third echo on, the film is superconducting. Thus the ratio of these echoes without and with the magnetic field yields α_s/α_n. The values obtained by this method are plotted as squares in Fig. 5 and agree well with the other methods for determining α_s. Note also that once the film becomes superconducting, the decay of the echoes becomes exponential, and the attenuation between successive echoes is the same as in the normal state.

III. COMPARISON OF EXPERIMENT WITH THEORY

To gain some physical insight we derive first the conversion efficiency of electromagnetic into acoustic energy due to diffuse surface scattering of electrons using a very simplified model. We consider a plane-polarized electromagnetic wave incident perpendicularly on a thin metal film. We assume that within the metal the electric field penetrates up to a penetration depth δ where its value suddenly drops to zero. We further assume that the conduction electrons are moving perpendicular to the film surface with a uniform velocity v_F and that scattering in the bulk can be neglected. Under these assumptions, the transverse momentum p_t acquired by an electron traversing the film is given by

$$p_t = -E_0 e \delta e^{-i\omega t}/v_F \ . \tag{1}$$

Here E_0 is the amplitude of the electric field at the surface, e is the absolute magnitude of the electronic charge, ω is the angular frequency, and $i = (-1)^{1/2}$. In Eq. (1) it was assumed that $\omega\tau < 1$, where τ is the scattering time (due mainly to surface scattering). The number of electrons per second striking a unit area of each surface is

$\frac{1}{2}n_0 v_F$, where n_0 is the density of conduction electrons. For diffuse surface scattering, the momentum acquired by the electrons from the field is transferred to the lattice at the surface. This momentum per unit time is equal to a shear force F_e given by

$$F_e = -\tfrac{1}{2}E_0 e\,\delta n_0\, e^{-i\omega t} \tag{2}$$

and generates a sound wave. The sound wave, originating at the surface, propagates in unit time to a distance v_s, where v_s is the sound velocity. Setting the momentum acquired by the ions equal to F_e we obtain

$$\rho v_s v_t = F_e\ , \tag{3}$$

where v_t is the average transverse velocity of the ions and ρ is the mass density. The acoustic flux w can be written as $w = \frac{1}{2}\rho v_s |v_t|^2$. The conversion efficiency α_e, due to diffuse scattering of electrons at one surface, is thus given by

$$\alpha_e = Aw/P = A|F_e|^2/2P\rho v_s\ , \tag{4}$$

where A is the area of the film and P is the microwave input power. We now express E_0 in Eq. (2) in terms of H_0, the amplitude of the magnetic field at the surface. For a propagating electromagnetic wave incident on a metal surface we have approximately $E_0 = H_0\omega/c\kappa$, where c is the velocity of light and κ is the (complex) propagation constant. We use also the value $|1/\kappa|$ for the penetration depth δ. Substituting now F_e from Eq. (2) into Eq. (4) and denoting the acoustic impedance ρv_s by Z_s, we obtain

$$\alpha_e = AH_0^2 e^2 n_0^2 \omega^2/8PZ_s c^2 |\kappa|^4\ . \tag{5}$$

Abeles[1] performed a more rigorous calculation of the conversion efficiency α. His main assumption is that the bulk electronic mean free path l is large compared to the film thickness d. To calculate F_e, Abeles integrates over the electrons striking the surface at different angles; only electrons whose trajectories originate at one surface and end at the opposite surface being considered. The integration is cut off at an angle θ_0, where $\cos\theta_0 = d/l$, i.e., only trajectories whose lengths are smaller than l are considered. The scattering in the bulk and the contribution of the electrons striking the surface at angles $\theta > \theta_0$ are neglected. This seems to be a reasonable approximation for $l \gg d$. In addition, it is assumed that the momentum transfer by the electrons to the surfaces is coherent. This assumption limits the theory to frequencies $\omega\tau < 1$, or to $l < v_F/\omega$, where v_F is the Fermi velocity of the electrons.

The transverse lattice displacement is derived from the standard wave equation which now also contains the direct electromagnetic force on the ions. The boundary conditions at the two surfaces include the shear stress F_e due to diffuse surface scattering. Assuming that the acoustic impedance of the metal film and the substrate are the same, Abeles[1] calculates the conversion efficiency as

$$\alpha = (\int H_0^2\, dA)\,(e^2 n_0^2 \omega^2/8PZ_s c^2 |\kappa|^4) G\ , \tag{6}$$

where

$$G = |1 + \cos qd - 2\kappa^2(1 - q\sin qd/\kappa\sin\kappa d)/(\kappa^2 - q^2)|^2\ . \tag{7}$$

The integration in Eq. (6) is performed over the area A of the film and q stands for the acoustic wave number. We see that apart from the factor G (and the integration over the area), α in Eq. (6) is identical with α_e given by Eq. (5).

In case the acoustic impedance Z_{s_1} of the metal film differs appreciably from that of the substrate Z_{s_2}, Eq. (6) has to be somewhat modified. A straightforward calculation along the lines of Abeles yields that Z_s has to be replaced by Z_s^*, where

$$Z_s^* = (Z_{s_1}^2 \sin^2 qd + Z_{s_2}^2 \cos^2 qd)/Z_{s_2}\ . \tag{8}$$

We now express H_0 in Eq. (6) in terms of P, the power absorbed in the cavity, and the quality factor Q. For a rectangular cavity with the TE_{101} mode we obtain approximately[10]

$$\frac{c}{8\pi P}\int H_0^2\, dA \approx \sqrt{2}\,\frac{A}{S}\,Q\ , \tag{9}$$

where S is the area of the bottom wall of the cavity. Introducing these into Eq. (6) we obtain

$$\alpha = (\sqrt{2}\,\pi A Q\omega^2 e^2 n_0^2/SZ_s^* c^3 |\kappa|^4) G\ . \tag{10}$$

The first two terms in the expression for G in Eq. (7) are due to diffuse surface scattering, while the rest is due to the direct force on the ions. The finite thickness of the film enters into Eq. (7) via the terms containing d. If we delete these terms, we indeed find that Abeles's result agrees with Southgate's[8] derived for a semi-infinite metal in the limit of long mean free path and diffuse surface scattering. If we neglect surface scattering, the first term in Eq. (7) disappears as well and G becomes equal to $|2\kappa^2/(\kappa^2 - q^2)|^2$. This again agrees with Southgate's calculation for the case of specular surface scattering.

Upon the transition into the superconducting state, Abeles[1] assumed that only normal electrons transfer momentum to the surface. Thus he multiplied F_e by the ratio n/n_0, defined as the fraction of the conduction electrons that can be scattered at the surface. Accordingly, the function G is modified to

$$G = |(n/n_0)(1 + \cos qd) - 2\kappa^2(1 - q\sin qd/\kappa\sin\kappa d)/(\kappa^2 - q^2)|^2\ . \tag{11}$$

A. Temperature Dependence

The electronic contribution to α is proportional to the fourth power of the penetration depth $|1/\kappa|$ and to $(n/n_0)^2$ [see Eqs. (10) and (11)]. Below the superconducting transition temperature $|1/\kappa|$ decreases with decreasing temperatures. In addition, if only normal electrons transfer momentum to the surface, n/n_0 decreases too. Thus the part of α due to surface scattering is expected to decrease rapidly below T_c. In the part of α due to the direct force on the ions, on the other hand, the $|1/\kappa|^4$ dependence cancels. Thus here, for $q^2 \gg |\kappa|^2$, the main temperature dependence arises from the last term in the expression for G.

To calculate the theoretical temperature dependence of α as given by Eqs. (10) and (11), we express κ in terms of the conductivity σ using the theory of skin effect. In the region of normal skin effect we obtain

$$\kappa_N = (4\pi i\omega\sigma/c^2)^{1/2} , \tag{12}$$

while in the extreme anomalous limit we obtain[8]

$$\kappa_A = (8\pi^2\omega\sigma/\sqrt{3}\, c^2 l)^{1/3} e^{i\pi/3} . \tag{13}$$

Equation (12) is expected to be a reasonable approximation at high temperatures, where $|1/\kappa| \gtrsim d$. At low T/T_c, $|1/\kappa|$ decreases towards the superconducting penetration depth λ and the anomalous limit would seem to be more appropriate. The temperature dependence of σ in the superconducting state was calculated from Mattis and Bardeen's theory[11] for σ/σ_n, where σ_n is the normal conductivity.

Before trying to fit the experimental data we first estimated the ionic contribution to α. We found that over the whole temperature range of our measurements this contribution is at least 17 dB below the experimental results (34- to 40-dB discrepancy in IL). For these calculations we assumed one conduction electron per atom, $n_0 = 3.8\times10^{22}$ cm^{-3}, and the value of $v_s = 1.3\times10^5$ cm/sec was derived from the measured[12] stiffness constant C_{66}. The value of κ was calculated from both Eqs. (12) and (13), and σ_n was obtained from the measured film conductivity σ_f, corrected[13] for diffuse surface scattering. In addition, we used the measured values of $Q \approx 6000$ and $d \approx 1200$ Å, and the estimated value of $l \approx 10\,000$ Å (for the anomalous limit).

Because of the negligible ionic contribution we calculated α using only the electronic contribution. These calculated values of α_s^2 are compared to the experimental data in Fig. 5. Curve N was calculated using Eq. (12) for κ_N (normal skin effect), while curves A were calculated for the extreme anomalous limit [Eq. (13)]. In calculating the two solid curves, we have taken the fraction of electrons, n/n_0, that can be scattered at the surface as 1. In calculating the dashed curve we assumed, according to the two-fluid model,[14] that $n/n_0 = (T/T_c)^4$. Inspecting Fig. 5, we see that the temperature dependence of the experimental data agrees well with the solid curve A, obtained for the anomalous limit and with $n/n_0 = 1$. Thus the whole temperature dependence of this curve arises from the temperature dependence of κ_A.

Because the anomalous limit becomes a better approximation the lower the temperature, we fitted (the solid) curve A to the experimental results at low temperatures. At higher temperatures the experimental data deviate somewhat from curve A and are bracketed by the two solid theoretical curves. This is expected because with increasing temperatures the approximation of the extreme anomalous limit becomes progressively worse.

The value of $|1/\kappa|$ was calculated from the measured values of α_s using Eq. (10). For samples whose thicknesses varied between 1100 and 1500 Å, our values for $|1/\kappa|$ at $T = 0.4T_c$ are between 600 and 650 Å. The value of the ratio σ_n/l obtained from Eq. (13) using the theory of Mattis and Bardeen[11] was $\sigma_n/l = (4.8\pm0.5)\times10^{10}\ \Omega^{-1}$ cm^{-2}. This agrees well with the value of σ_n obtained[13] for diffuse surface scattering from the measured film conductivity σ_f (around $10^6\ \Omega^{-1}$ cm^{-1}) and the estimated value of l ($\approx 10\,000$ Å).

B. Magnetic Field Dependence

In the range of our magnetic fields (up to 1 kOe), we found that above T_c, α was independent of the applied magnetic field H. Thus it is reasonable to assume that the field dependence of α below T_c is due solely to the transition of the indium film from the superconducting to the normal state. This is also evidenced by the fact that at sufficiently high fields the value of α always attained its value above T_c. The value of H necessary to restore the value of α_n was, however, microwave power dependent. We took the limiting values of H (in the limit of low microwave power) necessary to restore α_n as the critical transition field of the film, $H_c(T)$. The experimental values of $H_c(T)$ are plotted in Fig. 8. The values for perpendicular fields $H_{c\perp}$ are in good agreement with the theoretical values shown by the two curves. The theoretical values of $H_{c\perp}$ were calculated from the theory of Tinkham[9] for thin-film superconductors in a perpendicular magnetic field. The values of $\lambda_0(d)$, the thickness-dependent superconducting penetration depth at 0 K, obtained from such fits, vary between 670 and 740 Å.

IV. DISCUSSIONS

The conversion efficiencies obtained by us were about two orders of magnitude higher than those

measured by Abeles.[1] There are two main reasons for this. (i) We used high-Q cavities; the quantity $(c/8\pi P)\int H_0^2\,dA$ that represents the enhancement of the field in the cavity and was estimated by Abeles to be ten, was around 800–1000 for our cavities. (ii) We found that the conversion efficiency is a very sensitive function of the quality of the contact between the cavity wall and the indium film. In addition, our maximum microwave input power was more than an order of magnitude above that reported by Abeles.

Because of our high conversion efficiencies and our higher powers we were able to study the temperature dependence of α down to $0.4T_c$. Good agreement was found between experiment and theory[1] with respect to both the value and the temperature dependence of α. To fit the temperature dependence of α below T_c we had to assume that the fraction of conduction electrons that can be scattered at the surface n/n_0 is equal to 1. This was quite a surprising result and we made heuristic efforts to fit the experimental results assuming specular surface scattering, at least for Cooper pairs below T_c. The parameter that we tried to vary was the propagation constant κ. However, the electronic contribution to α depends on $|1/\kappa|^4$ and, if we assume diffuse surface scattering above T_c, the value of $|\kappa|$ is fixed by the experimental results within a very small margin. Thus to be able to vary κ we had to assume specular surface scattering above T_c as well. To explain the experimental data by the ionic contribution alone we had to assume a value for $|\kappa|$ above that of q $(=4.35\times10^5\ \mathrm{cm}^{-1})$. This leads immediately to two difficulties. First, such a high value of $|\kappa|$ indicates a ridiculously small electromagnetic penetration depth (≈ 200 Å) above T_c and an enormous value for the conductivity of our films. Second, the calculated temperature dependence of α_s^2, using such a high $|\kappa|$, shows a decrease of over seven orders of magnitude as compared to the experimentally observed decrease of four orders of magnitude.

Assuming diffuse surface scattering below T_c as well, the observed temperature dependence of α agrees well with the theory. Under this assumption also the value of $|1/\kappa|$ at low temperatures is in reasonable agreement with the values for the superconducting penetration depth of indium published in the literature.[1,15,16] It is also in good agreement with the measured conductivity of our films above T_c. The temperature dependence of the critical (perpendicular) magnetic field of our films provided another, independent, method for determining the thickness-dependent penetration depth $\lambda_0(d)$. The values of λ derived[17] from $\lambda_0(d)$ are also in reasonable agreement with those derived from $|1/\kappa|$.

The theory implies a resonant $(1+\cos qd)$ behavior as a function of the film thickness d. For maximum sensitivity we tried to prepare samples whose thicknesses were around the resonant thickness ($qd=2\pi$, $d=1440$ Å). However, we find that for the case of indium films on silicon substrates, the thickness of the film is not critical and that α is almost independent of d around the resonant thickness. This is shown in Fig. 11 where we plotted the calculated values of IL(α^2) as a function of qd. The values of d are also marked on the top of the diagram. For the calculation we used the value of 5.85×10^5 cm sec^{-1} for the sound velocity in silicon. This is appropriate for propagation along the [100] direction and for the fast shear mode along the [110] direction. The figure shows the values of IL (in dB) relative to its maximum value (resonant thickness). The reason that IL varies so slowly with d is the thickness dependence of Z_s^* [see Eq. (8)], which greatly reduces the $(1+\cos qd)$ dependence.

We did not try to verify experimentally the theoretical dependence of α on qd. One way of doing this would be to compare the values of α for films of different thicknesses. However, we felt that the accuracy of this method would be poor because (as already pointed out) α is very sensitive to the quality of the contact between the film and the cavity wall. Another method would be to work with the same film (fixed d) and vary the acoustic wave number q. Because the frequency of the microwave cavity can be varied only by a few percent, to vary $\cos qd$ appreciably, one has to employ films several acoustic wavelengths thick. However, for such thick films the assumptions of the theory, leading to the $(1+\cos qd)$ term, break down. This term results directly from the assumption that the film is thin and because of that the electrons striking each surface originate at the opposite surface. Thus all the electrons pass through the

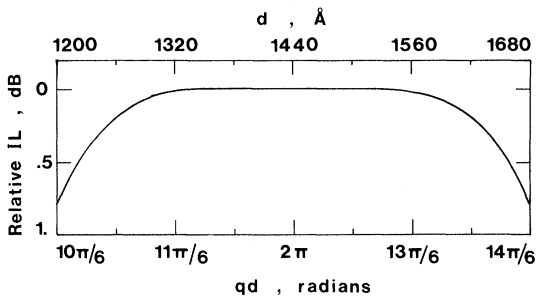

FIG. 11. Calculated values of IL $(=\alpha^2)$ for indium on silicon substrates (propagation along the [100] or fast shear wave along the [110] direction) relative to its maximum value as a function of qd. The values of d are also marked on the top of the figure.

same field and the transfer of electronic momentum to both surfaces is symmetrical. For a thick film this assumption is no longer valid and most of the electrons striking the back surface originate within the field-free volume of the film. The momentum transfer to the back surface is thus greatly reduced and $\cos qd$ should be multiplied by an attenuation factor. This is probably the reason why Weisbarth[18] was not able to detect a $(1+\cos qd)$ behavior with thick films.

The microwave power dependence of α below T_c is one of the striking experimental results. On the basis of the available experimental evidence we interpret this power dependence as due to the transition of the indium film from the superconducting into the normal state under the influence of the electromagnetic radiation. This interpretation is also consistent with the results on the power and echo number dependence of the critical magnetic field. Thus, while there is little doubt in our minds that the interpretation is correct, we are not quite sure of the exact mechanism of this quenching. The obvious mechanism would be the quenching of the indium film by the microwave magnetic field. However, it seems to us that this mechanism by itself cannot explain the experimental results. We estimate the amplitude of the microwave magnetic field in the cavity for the highest powers used as 80–90 Oe. As can be seen from the values of $H_{c\parallel}$ in Fig. 8, this field seems to be insufficient to quench the indium film below about $0.9T_c$. An additional difficulty would be to explain, as due to this field, the quenching of the film at the time of the first echoes (as often observed experimentally). Thus an additional mechanism is necessary to explain the quenching at high and intermediate microwave powers. We think that this additional mechanism is possibly the heating of the film by the high-power microwave pulse. The heating can be due to power absorption by the film but more probably due to power dissipation across the contact between the indium film and the cavity wall. This seems to be indicated by the fact that samples whose contact with the cavity was not so good could be quenched by the microwave power at quite low reduced temperatures.

V. CONCLUSIONS

The good agreement between our results and the theory of Abeles[1] shows that at our frequencies the generation of the acoustic waves is due primarily to diffuse surface scattering of the conduction electrons. Furthermore, to fit the theory to the experiment we had to assume that $n/n_0 = 1$, and thus we conclude that superconducting pair scattering at the surface does not conserve momentum. This somewhat surprising conclusion is in agreement with our previous results[19] and with results of microwave absorption experiments.[20,21]

The conversion efficiencies found above T_c are quite high and comparable with those obtained using quartz transducers. Thus we find that in some applications indium films may serve as transducers for generating hypersonic waves. Below T_c, α_s decreases rapidly but a small (perpendicular) magnetic field is able to restore its value to α_n.

Our experimental results show that the value of α_s is appreciable even at low reduced temperatures. Thus transverse-phonon generation may very well be one of the important loss mechanisms that may account for the observed[22] losses in very-high-Q superconducting cavities. In the case of indium, for example, the residual microwave surface resistance at 9 GHz due to this mechanism is calculated to be $1-2\times10^{-7}$ Ω.

*Work supported in part by The Central Research Fund of the Hebrew University of Jerusalem.

[1]B. Abeles, Phys. Rev. Letters 19, 1181 (1967).
[2]Y. Goldstein and A. Zemel, Phys. Rev. Letters 28, 147 (1972).
[3]M. I. Kaganov and V. B. Fiks, Fiz. Metal. i Metalloved 19, 489 (1965) [Phys. Metals Metallog. (USSR) 19, 8 (1965)].
[4]J. J. Quinn, Phys. Letters 25A, 522 (1967).
[5]R. C. Alig, Phys. Rev. 178, 1050 (1969).
[6]J. Halbritter, J. Appl. Phys. 42, 82 (1971).
[7]C. Passow, Phys. Rev. Letters 28, 427 (1972).
[8]P. D. Southgate, J. Appl. Phys. 40, 22 (1969).
[9]M. Tinkham, Phys. Rev. 129, 2413 (1963).
[10]See, for example, *American Institute of Physics Handbook*, 2nd ed., edited by Dwight E. Gray (McGraw-Hill, New York, 1972), pp. 5–65.
[11]D. C. Mattis and J. Bardeen, Phys. Rev. 111, 412 (1958).
[12]D. R. Wider and C. S. Smith, J. Phys. Chem. Solids 4, 128 (1958).
[13]See, for example, A. H. Wilson, *The Theory of Metals*, 2nd ed. (Cambridge U. P., Cambridge, England, 1953), p. 245.
[14]M. Tinkham, in *Low-Temperature Physics*, edited by C. Dewitt, B. Dreyfus, and P. G. de Gennes (Gordon and Breach, New York, 1962).
[15]A. M. Toxen, Phys. Rev. 127, 382 (1962).
[16]J. I. Gittleman, S. Bozowski, and B. Rosenblum, Phys. Rev. 161, 398 (1967).
[17]M. Tinkham, as cited by G. D. Cody and R. E. Miller, Phys. Rev. 173, 481 (1968), Eq. (4).
[18]G. S. Weisbarth, Phys. Letters 27A, 230 (1968).
[19]Y. Goldstein and B. Abeles, in *Proceedings of the Eleventh International Conference on Low Temperature Physics*, edited by J. F. Allen *et al.* (University of St. Andrews Printing Department, St. Andrews, Scotland, 1968), p. 965.
[20]W. V. Budzinski and M. P. Garfunkel, in *Proceedings of the Tenth International Conference on Low Temperature Physics, Moscow*, 1966, edited by M. P. Malkov (VINITI, Moscow, 1967), Vol. IIB, p. 243.
[21]G. Fischer and R. Klein, Phys. Rev. 165, 578 (1968).
[22]See, for example, the summaries of experimental results on residual rf losses in superconducting cavities in Refs. 6 and 7.

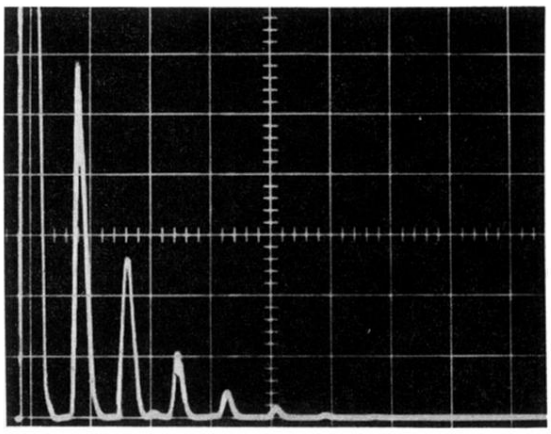

FIG. 1. Typical oscillogram of echoes detected by the superheterodyne receiver above T_c. Horizontal scale, 5 μsec/division.